Journal of Molecular Structure 918 (2009) 108–115

Contents lists available at ScienceDirect

Journal of Molecular Structure

journal homepage: www.elsevier.com/locate/molstruc

Structural and spectroscopic studies of a new 2-naphthylmethyl ester of lasalocid acid

Adam Huczyński [a], Izabela Paluch [a], Małgorzata Ratajczak-Sitarz [a], Andrzej Katrusiak [a], Bogumil Brzezinski [a,*], Franz Bartl [b]

[a] Faculty of Chemistry, Adam Mickiewicz University, Grunwaldzka 6, 60-780 Poznan, Poland
[b] Institute of Medical Physics and Biophysics Charité, Universitätsmedizin Berlin Campus, Charité Mitte, Ziegelstr. 5/9, 10117 Berlin, Germany

ARTICLE INFO

Article history:
Received 16 June 2008
Accepted 21 July 2008
Available online 3 August 2008

Keywords:
Ionophores
Lasalocid ester
X-ray
Spectroscopic methods
PM5 calculation

ABSTRACT

A new lasalocid 2-naphthylmethyl ester (NAFB) has been synthesised and studied by X-ray, ^{1}H NMR, ^{13}C NMR, FT-IR, UV–vis, fluorescence-spectroscopy as well as by the PM5 semiempirical method. The crystals of NAFB are monoclinic, space group $P2_1$ with $a = 10.120(2)$ Å, $b = 18.245(3)$ Å, $c = 12.354(3)$ Å, $\beta = 109.65(3)^{\circ}$ and $Z = 2$. The molecular conformation of NAFB in the solid state is stabilized by three intramolecular hydrogen bonds, and no intermolecular H-bonds are formed. The FT-IR spectrum of NAFB in chloroform indicates equilibrium between two NAFB conformers. In the first conformer the keto group forms an intramolecular hydrogen bond, while in the second one this group is not involved in any hydrogen bonds. The two structures of NAFB are calculated by the PM5 method and discussed in detail.

1. Introduction

Ionophores are biologically interesting groups of compounds capable of transporting various cations across biological membranes [1–11]. Lasalocid isolated from *Streptomyces lasaliensis* is a representative of these compounds. It has important and useful biological activities such as the growth inhibition of the Gram-positive bacteria and the effective control of coccidiosis in chickens, beef and cattle [12–17].

Recently, some esters of lasalocid, in particular those with polyoxaalkyl chains or aromatic substituents have been synthesised and their structures have been studied by different methods [18–24]. According to the results of these papers, the increasing length of the oxaalkyl chains of the respective derivatives results in an enhanced effectiveness of the complexation process of the monovalent cations. For the esters with aromatic substituents no influence of these rings on the complexation process was observed.

Crucial points for the biological activity of these compounds are molecular conformation and intermolecular interactions. In this paper we report the structures of a new lasalocid 2-naphthylmethyl ester (Scheme 1) in the solid state and in the solution as elucidated by X-ray crystallography, FT-IR, ^{1}H NMR, ^{13}C NMR, UV–vis, fluorescence-spectroscopy and PM5 methods.

2. Experimental

2.1. Preparation lasalocid 2-naphthylmethyl ester (NAFB)

Lasalocid sodium salt was extracted from Avatec (Fa. Spezialfutter Neuruppin). It was dissolved in dichloromethane and stirred vigorously with a layer of diluted aqueous sulphuric acid (pH = 1.5). The organic layer containing lasalocid acid was washed with distilled water. Subsequently dichloromethane was evaporated under reduced pressure to dryness.

A mixture of 2-(bromomethyl)naphthalene (221 mg, 1.00 mmol, Fluka), LAS (500 mg, 0.85 mmol) and 1,8-diazabicyclo[5.4.0]undec-7-en (DBU) (130 mg, 0.85 mmol) and 40 ml toluene was heated at 90 °C for 5 h. After cooling, the precipitate DBU-hydrobromide (DBU•HBr) was filtered and washed with hexane. Hexane was evaporated under reduced pressure and the residue was purified by chromatography on silica gel (Fluka type 60) yielding NAFB (343 mg, 55% yield, m.p. 97 °C). The crystals of NAFB were obtained by crystallization from dried acetonitrile solutions.

Elemental analysis: Calculated: C 73.94%; H 8.55%, Found: C 73.79%; H 8.71%.

2.2. X-ray measurements

The crystals selected for single-crystal X-ray diffraction measurements formed colourless parallelepipeds with well-developed faces. They were stable under normal conditions and the X-ray diffraction measurements were carried out on a Kuma KM-4 CCD

* Corresponding author. Tel.: +48 618291330.
E-mail address: bbrzez@main.amu.edu.pl (B. Brzezinski).

0022-2860/$ - see front matter © 2008 Elsevier B.V. All rights reserved.
doi:10.1016/j.molstruc.2008.07.024

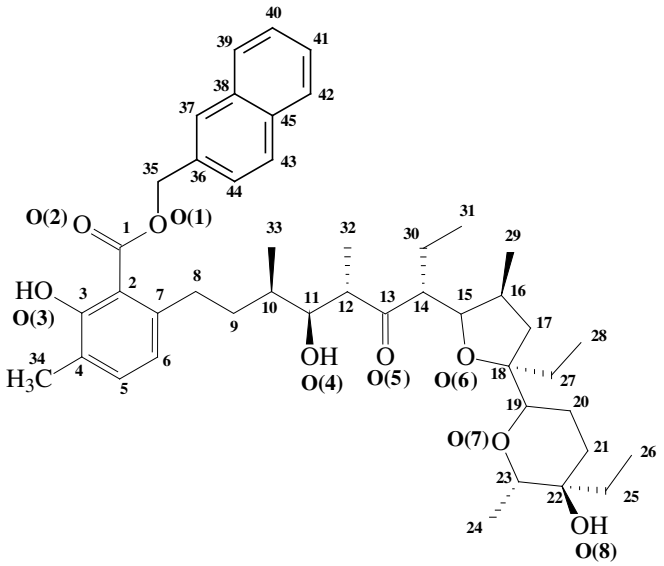

Scheme 1. The structures and atom numbering of NAFB.

diffractometer at 296 K. The structure was solved by direct methods [25] and refined by full-matrix least-squares [26]. The positions of all H-atoms were determined on the basis of the molecular geometry (C–H 0.93–0.98, O–H 0.82 Å) and recalculated after each refinement cycle. U_{iso}'s were related to the thermal vibrations of their carriers. The absolute conformation of NAFB in the crystal was consistent with the chemical information. Selected details about the crystal structure, experiment and structure solution and refinement are given in Table 1. The fractional atomic coordinates are listed in Table 2. The crystallographic-information-file (CIF) has been deposited at the Cambridge Crystallographic Database Centre as a Supplementary Publication No. CCDC 688478.

2.3. NMR measurements

The NMR spectra were recorded in $CDCl_3$ using a Varian Gemini 300 MHz spectrometer. All spectra were locked to deuterium resonance of $CDCl_3$. The error in ppm values was 0.01. All ^1H NMR measurements were carried out at the operating frequency 300.075 MHz; flip angle, pw = 45°; spectral width, sw = 4500 Hz; acquisition time, at = 2.0 s; relaxation delay, d_1 = 1.0 s; T = 293.0 K and TMS as the internal standard. No window function or zero filling was used. Digital resolution was 0.2 Hz/point. ^{13}C NMR spectra were recorded at the operating frequency 75.454 MHz; pw = 60°; sw = 19,000 Hz; at = 1.8 s; d_1 = 1.0 s; T = 293.0 K and TMS as the internal standard.

The ^1H and ^{13}C NMR signals were assigned independently for each species using one or two-dimensional (COSY, HETCOR) spectra.

2.4. FT-IR measurements

In the mid infrared region the FT-IR spectra of NAFB were recorded in chloroform solution and potassium bromide in the

Table 1
Crystal data and structure refinement

Empirical formula	$C_{45}H_{62}O_8$
Formula weight	730.95
Temperature (K)	293(2)
Wavelength (Å)	0.71073
Crystal system, space group	Monoclinic, $P2_1$
Unit cell dimensions	
a (Å)	10.120(2)
b (Å)	18.245(3)
c (Å)	12.354(3)
β (°)	109.65(3)
Volume (Å^3)	2148.2(8)
Z	2
Calculated density (g cm^{-3})	1.130
Absorption coefficient (mm^{-1})	0.076
$F(000)$	792
Crystal size (mm)	0.30 × 0.20 × 0.075
θ Range for data collection (°)	2.14–29.85
Limiting indices	$-13 \leqslant h \leqslant 13$, $-23 \leqslant k \leqslant 24$, $-17 \leqslant l \leqslant 16$
Reflections collected/unique	29,068/10,641 R_{int} = 0.1206
Completeness to θ = 29.85 (%)	90.7
Refinement method	Full-matrix least-squares on F^2
Data/restraints/parameters	10641/1/478
Goodness-of-fit on F^2	0.796
Final R indices [$I > 2\sigma(I)$]	R_1 = 0.0494, wR_2 = 0.0480
R indices (all data)	R_1 = 0.3316, wR_2 = 0.0626
Absolute structure parameter	−0.4(9)
Largest diff. peak and hole (e Å^{-3})	0.224 and −0.204

Table 2
Atomic coordinates (× 10^4) and equivalent isotropic displacement parameters (Å^2 × 10^3)

	x	y	z	U(eq)
O(1)	8201(4)	7764(2)	3421(4)	112(1)
O(2)	10064(5)	7839(3)	5016(4)	182(2)
O(3)	10340(4)	6950(2)	6625(3)	140(2)
O(4)	7268(3)	7555(2)	530(2)	83(1)
O(5)	4225(3)	8329(2)	−456(3)	90(1)
O(6)	6779(4)	8618(2)	−1324(3)	83(1)
O(7)	9560(4)	8778(2)	411(4)	86(1)
O(8)	10259(3)	7381(2)	1509(2)	93(1)
C(1)	8988(8)	7536(4)	4434(6)	98(2)
C(2)	8528(7)	6822(3)	4773(6)	78(2)
C(3)	9249(6)	6576(4)	5931(6)	93(2)
C(4)	8861(8)	5938(4)	6363(6)	100(2)
C(5)	7753(8)	5556(3)	5688(7)	108(2)
C(6)	7047(6)	5776(3)	4539(6)	108(2)
C(7)	7391(7)	6414(3)	4087(5)	76(2)
C(8)	6539(4)	6549(2)	2840(4)	83(2)
C(9)	7358(4)	6308(2)	2024(4)	77(1)
C(10)	6489(5)	6344(3)	729(4)	68(1)
C(11)	6039(5)	7114(3)	335(4)	70(1)
C(12)	5056(5)	7167(2)	−924(4)	73(1)
C(13)	4515(5)	7961(3)	−1144(5)	73(2)
C(14)	4365(5)	8256(3)	−2365(4)	84(2)
C(15)	5863(6)	8323(3)	−2393(5)	92(2)
C(16)	6147(6)	8832(3)	−3302(5)	103(2)
C(17)	7682(5)	8998(3)	−2782(5)	113(2)
C(18)	7922(6)	9045(3)	−1477(5)	85(2)
C(19)	9314(5)	8677(3)	−770(5)	76(2)
C(20)	9444(5)	7881(3)	−1025(4)	89(2)
C(21)	10842(5)	7599(2)	−227(5)	88(2)
C(22)	11167(6)	7766(3)	1032(5)	83(2)
C(23)	10923(5)	8600(3)	1169(4)	92(2)
C(24)	12061(4)	9130(2)	978(4)	119(2)
C(25)	12671(5)	7504(4)	1733(5)	143(2)
C(26)	13066(6)	7735(4)	2890(5)	167(3)
C(27)	7651(7)	9828(3)	−1071(7)	174(3)
C(28)	8712(8)	10269(4)	−1074(7)	291(5)
C(29)	5679(5)	8454(4)	−4514(5)	174(3)
C(30)	3534(5)	8999(3)	−2585(4)	111(2)
C(31)	2018(5)	8910(3)	−2691(4)	138(2)
C(32)	3720(4)	6647(2)	−1219(3)	90(2)
C(33)	7312(5)	5950(2)	61(4)	102(2)
C(34)	9754(6)	5693(3)	7618(4)	157(3)
C(35)	8707(6)	8428(3)	3034(4)	141(3)
C(36)	8023(10)	9091(4)	3362(7)	93(2)
C(37)	8668(6)	9525(4)	4233(6)	94(2)
C(38)	7923(12)	10197(4)	4443(8)	103(2)
C(39)	8586(8)	10632(6)	5346(7)	150(3)
C(40)	7856(15)	11264(5)	5509(9)	200(5)
C(41)	6423(16)	11355(8)	4740(12)	225(7)
C(42)	5695(16)	10935(6)	3936(11)	221(7)
C(43)	5908(10)	9830(7)	2865(9)	166(4)
C(44)	6602(13)	9220(5)	2637(8)	145(4)
C(45)	6528(12)	10269(5)	3758(9)	112(2)

U(eq) is defined as one third of the trace of the orthogonalized U_{ij} tensor.

Table 3
Bond lengths (Å) and angles (°)

O(1)–C(1)	1.305(6)
O(1)–C(35)	1.457(5)
O(2)–C(1)	1.218(6)
O(3)–C(3)	1.335(5)
O(4)–C(11)	1.432(4)
O(5)–C(13)	1.194(5)
O(6)–C(15)	1.439(4)
O(6)–C(18)	1.460(5)
O(7)–C(19)	1.408(4)
O(7)–C(23)	1.420(5)
O(8)–C(22)	1.431(5)
C(1)–C(2)	1.490(8)
C(2)–C(7)	1.393(6)
C(2)–C(3)	1.442(6)
C(3)–C(4)	1.391(6)
C(4)–C(5)	1.346(6)
C(4)–C(34)	1.574(6)
C(5)–C(6)	1.416(6)
C(6)–C(7)	1.385(5)
C(7)–C(8)	1.511(5)
C(8)–C(9)	1.569(5)
C(9)–C(10)	1.546(5)
C(10)–C(11)	1.506(5)
C(10)–C(33)	1.534(5)
C(11)–C(12)	1.541(5)
C(12)–C(13)	1.540(6)
C(12)–C(32)	1.590(4)
C(13)–C(14)	1.561(6)
C(14)–C(15)	1.532(5)
C(14)–C(30)	1.569(5)
C(15)–C(16)	1.557(6)
C(16)–C(17)	1.499(5)
C(16)–C(29)	1.571(6)
C(17)–C(18)	1.550(5)
C(18)–C(19)	1.540(5)
C(18)–C(27)	1.568(7)
C(19)–C(20)	1.501(5)
C(20)–C(21)	1.516(5)
C(21)–C(22)	1.508(6)
C(22)–C(25)	1.551(6)
C(22)–C(23)	1.562(6)
C(23)–C(24)	1.580(5)
C(25)–C(26)	1.413(6)
C(27)–C(28)	1.343(8)
C(30)–C(31)	1.504(4)
C(35)–C(36)	1.515(7)
C(36)–C(37)	1.319(6)
C(36)–C(44)	1.435(9)
C(37)–C(38)	1.506(7)
C(38)–C(39)	1.349(8)
C(38)–C(45)	1.387(7)
C(39)–C(40)	1.420(9)
C(40)–C(41)	1.451(13)
C(41)–C(42)	1.274(13)
C(42)–C(45)	1.536(13)
C(43)–C(45)	1.337(8)
C(43)–C(44)	1.394(9)
C(1)–O(1)–C(35)	114.3(6)
C(15)–O(6)–C(18)	112.0(4)
C(19)–O(7)–C(23)	116.6(4)
O(2)–C(1)–O(1)	123.9(7)
O(2)–C(1)–C(2)	122.3(7)
O(1)–C(1)–C(2)	113.6(7)
C(7)–C(2)–C(3)	118.5(6)
C(7)–C(2)–C(1)	124.6(7)
C(3)–C(2)–C(1)	116.7(6)
O(3)–C(3)–C(4)	117.4(8)
O(3)–C(3)–C(2)	120.8(6)
C(4)–C(3)–C(2)	121.8(6)
C(5)–C(4)–C(3)	118.7(7)
C(5)–C(4)–C(34)	123.1(7)
C(3)–C(4)–C(34)	118.2(7)
C(4)–C(5)–C(6)	120.6(6)
C(7)–C(6)–C(5)	122.2(6)
C(6)–C(7)–C(2)	118.1(6)
C(6)–C(7)–C(8)	114.4(6)
C(2)–C(7)–C(8)	127.2(6)
C(7)–C(8)–C(9)	111.5(4)
C(10)–C(9)–C(8)	114.4(4)
C(11)–C(10)–C(33)	115.0(4)
C(11)–C(10)–C(9)	112.3(4)
C(33)–C(10)–C(9)	108.3(4)
O(4)–C(11)–C(10)	108.6(4)
O(4)–C(11)–C(12)	111.4(4)
C(10)–C(11)–C(12)	114.0(4)
C(13)–C(12)–C(11)	107.9(4)
C(13)–C(12)–C(32)	107.2(4)
C(11)–C(12)–C(32)	113.9(4)
O(5)–C(13)–C(12)	124.1(5)
O(5)–C(13)–C(14)	121.8(5)
C(12)–C(13)–C(14)	114.1(5)
C(15)–C(14)–C(13)	105.9(4)
C(15)–C(14)–C(30)	113.8(4)
C(13)–C(14)–C(30)	109.7(4)
O(6)–C(15)–C(14)	110.3(4)
O(6)–C(15)–C(16)	102.8(4)
C(14)–C(15)–C(16)	119.2(5)
C(17)–C(16)–C(15)	103.2(5)
C(17)–C(16)–C(29)	115.7(5)
C(15)–C(16)–C(29)	110.9(5)
C(16)–C(17)–C(18)	103.5(4)
O(6)–C(18)–C(19)	107.9(4)
O(6)–C(18)–C(17)	104.6(4)
C(19)–C(18)–C(17)	111.0(5)
O(6)–C(18)–C(27)	102.3(5)
C(19)–C(18)–C(27)	116.2(5)
C(17)–C(18)–C(27)	113.6(5)
O(7)–C(19)–C(20)	110.3(4)
O(7)–C(19)–C(18)	109.8(5)
C(20)–C(19)–C(18)	115.6(5)
C(19)–C(20)–C(21)	108.7(5)
C(22)–C(21)–C(20)	115.7(4)
O(8)–C(22)–C(21)	112.2(4)
O(8)–C(22)–C(25)	105.4(4)
C(21)–C(22)–C(25)	110.3(5)
O(8)–C(22)–C(23)	106.6(4)
C(21)–C(22)–C(23)	108.7(4)
C(25)–C(22)–C(23)	113.6(5)
O(7)–C(23)–C(22)	107.8(4)
O(7)–C(23)–C(24)	110.9(4)
C(22)–C(23)–C(24)	115.5(4)
C(26)–C(25)–C(22)	111.4(6)
C(28)–C(27)–C(18)	108.6(8)
C(31)–C(30)–C(14)	113.2(4)
O(1)–C(35)–C(36)	109.5(4)
C(37)–C(36)–C(44)	121.8(8)
C(37)–C(36)–C(35)	123.6(8)
C(44)–C(36)–C(35)	114.6(9)
C(36)–C(37)–C(38)	119.4(7)
C(39)–C(38)–C(45)	124.7(10)
C(39)–C(38)–C(37)	118.9(11)
C(45)–C(38)–C(37)	115.9(8)
C(38)–C(39)–C(40)	117.2(9)
C(39)–C(40)–C(41)	116.9(12)
C(42)–C(41)–C(40)	129(2)
C(41)–C(42)–C(45)	112.7(19)
C(45)–C(43)–C(44)	121.1(11)
C(43)–C(44)–C(36)	118.1(10)
C(43)–C(45)–C(38)	123.1(9)
C(43)–C(45)–C(42)	117.7(13)
C(38)–C(45)–C(42)	118.9(11)

form of pellets. A cell with Si windows and wedge-shaped layers was used to avoid interferences (mean layer thickness 170 μm). The spectra were taken with an IFS 113v FT-IR spectrophotometer (Bruker, Karlsruhe) equipped with a DTGS detector; resolution 2 cm^{-1}, NSS = 64. The Happ–Genzel apodization function was used.

2.5. UV–vis and fluorescence measurements

The absorption spectra of LAS and NAFB were recorded in 1 cm cells on a Jasco V-550 spectrophotometer (JASCO, Tokyo, Japan).

Table 4
Selected torsion angles (°)

C(35)–O(1)–C(1)–O(2)	−0.7(9)
C(35)–O(1)–C(1)–C(2)	−174.9(4)
O(2)–C(1)–C(2)–C(7)	−173.0(6)
O(1)–C(1)–C(2)–C(7)	1.3(7)
O(2)–C(1)–C(2)–C(3)	12.5(8)
O(1)–C(1)–C(2)–C(3)	−173.2(5)
C(7)–C(2)–C(3)–O(3)	−179.6(5)
C(1)–C(2)–C(3)–O(3)	−4.7(7)
C(1)–C(2)–C(3)–C(4)	176.5(5)
O(3)–C(3)–C(4)–C(5)	179.1(5)
O(3)–C(3)–C(4)–C(34)	−1.6(7)
C(2)–C(3)–C(4)–C(34)	177.2(4)
C(34)–C(4)–C(5)–C(6)	−175.7(5)
C(5)–C(6)–C(7)–C(8)	178.9(5)
C(1)–C(2)–C(7)–C(6)	−177.0(5)
C(3)–C(2)–C(7)–C(8)	−176.6(4)
C(1)–C(2)–C(7)–C(8)	9.0(8)
C(6)–C(7)–C(8)–C(9)	−98.8(5)
C(2)–C(7)–C(8)–C(9)	75.4(6)
C(7)–C(8)–C(9)–C(10)	173.2(4)
C(8)–C(9)–C(10)–C(11)	63.3(5)
C(8)–C(9)–C(10)–C(33)	−168.7(3)
C(33)–C(10)–C(11)–O(4)	−63.8(5)
C(9)–C(10)–C(11)–O(4)	60.6(5)
C(33)–C(10)–C(11)–C(12)	61.0(5)
C(9)–C(10)–C(11)–C(12)	−174.6(3)
O(4)–C(11)–C(12)–C(13)	−65.1(5)
C(10)–C(11)–C(12)–C(13)	171.7(4)
O(4)–C(11)–C(12)–C(32)	176.1(3)
C(10)–C(11)–C(12)–C(32)	52.8(5)
C(11)–C(12)–C(13)–O(5)	−37.5(6)
C(32)–C(12)–C(13)–O(5)	85.6(6)
C(11)–C(12)–C(13)–C(14)	142.7(4)
C(32)–C(12)–C(13)–C(14)	−94.3(4)
O(5)–C(13)–C(14)–C(15)	112.1(6)
C(12)–C(13)–C(14)–C(15)	−68.0(5)
O(5)–C(13)–C(14)–C(30)	−11.1(7)
C(12)–C(13)–C(14)–C(30)	168.7(4)
C(18)–O(6)–C(15)–C(14)	−149.4(4)
C(18)–O(6)–C(15)–C(16)	−21.3(5)
C(13)–C(14)–C(15)–O(6)	−41.4(5)
C(30)–C(14)–C(15)–O(6)	79.2(5)
C(13)–C(14)–C(15)–C(16)	−159.9(5)
C(30)–C(14)–C(15)–C(16)	−39.3(7)
O(6)–C(15)–C(16)–C(17)	35.4(5)
C(14)–C(15)–C(16)–C(17)	157.6(5)
O(6)–C(15)–C(16)–C(29)	159.8(4)
C(14)–C(15)–C(16)–C(29)	−77.9(6)
C(15)–C(16)–C(17)–C(18)	−35.8(5)
C(29)–C(16)–C(17)–C(18)	−157.0(5)
C(15)–O(6)–C(18)–C(19)	−118.9(5)
C(15)–O(6)–C(18)–C(17)	−0.7(6)
C(15)–O(6)–C(18)–C(27)	118.0(5)
C(16)–C(17)–C(18)–O(6)	23.4(6)
C(16)–C(17)–C(18)–C(19)	139.4(5)
C(16)–C(17)–C(18)–C(27)	−87.4(5)
C(23)–O(7)–C(19)–C(20)	63.6(5)
C(23)–O(7)–C(19)–C(18)	−167.8(4)
O(6)–C(18)–C(19)–O(7)	−70.6(5)
C(17)–C(18)–C(19)–O(7)	175.4(4)
C(27)–C(18)–C(19)–O(7)	43.5(6)
O(6)–C(18)–C(19)–C(20)	54.9(6)
C(17)–C(18)–C(19)–C(20)	−59.1(6)
C(27)–C(18)–C(19)–C(20)	169.1(5)
O(7)–C(19)–C(20)–C(21)	−52.5(5)
C(18)–C(19)–C(20)–C(21)	−177.8(4)
C(19)–C(20)–C(21)–C(22)	50.2(5)
C(20)–C(21)–C(22)–O(8)	67.6(5)
C(20)–C(21)–C(22)–C(25)	−175.3(4)
C(20)–C(21)–C(22)–C(23)	−50.1(6)
C(19)–O(7)–C(23)–C(22)	−62.1(5)
C(19)–O(7)–C(23)–C(24)	65.2(5)
O(8)–C(22)–C(23)–O(7)	−69.5(5)
C(21)–C(22)–C(23)–O(7)	51.7(5)
C(25)–C(22)–C(23)–O(7)	174.9(4)
O(8)–C(22)–C(23)–C(24)	165.9(4)
C(21)–C(22)–C(23)–C(24)	−72.9(5)
C(25)–C(22)–C(23)–C(24)	50.3(7)

Table 4 (*continued*)

O(8)–C(22)–C(25)–C(26)	−66.0(7)
C(21)–C(22)–C(25)–C(26)	172.7(5)
C(23)–C(22)–C(25)–C(26)	50.3(7)
O(6)–C(18)–C(27)–C(28)	174.7(7)
C(19)–C(18)–C(27)–C(28)	57.5(9)
C(17)–C(18)–C(27)–C(28)	−73.2(9)
C(15)–C(14)–C(30)–C(31)	173.3(4)
C(13)–C(14)–C(30)–C(31)	−68.2(5)
C(1)–O(1)–C(35)–C(36)	−93.1(7)
O(1)–C(35)–C(36)–C(37)	103.2(6)
O(1)–C(35)–C(36)–C(44)	−77.4(6)
C(35)–C(36)–C(37)–C(38)	176.3(5)
C(35)–C(36)–C(44)–C(43)	−178.5(6)

The UV–vis spectra of LAS and NAFB (1×10^{-5} mol dm^{-3}) were recorded for these compounds in spectral–grade. The intensity of fluorescence emission was measured for LAS and NAFB at the angle 90° relative to the incident excitation light. During the absorption and fluorescence measurements the samples were kept at room temperature. The samples were excited at 260 nm. The fluorescence quantum yield of NAFB was estimated from the equation:

$$\Phi^S = \Phi^R \cdot \frac{A^R}{F^R} \cdot \frac{F^S}{A^S} \left(\frac{n^S}{n^R}\right)^2$$

where Φ^R is the quantum yield of the standard, A is the absorbance at the wavelength of the excitation, F is the integrated intensity of

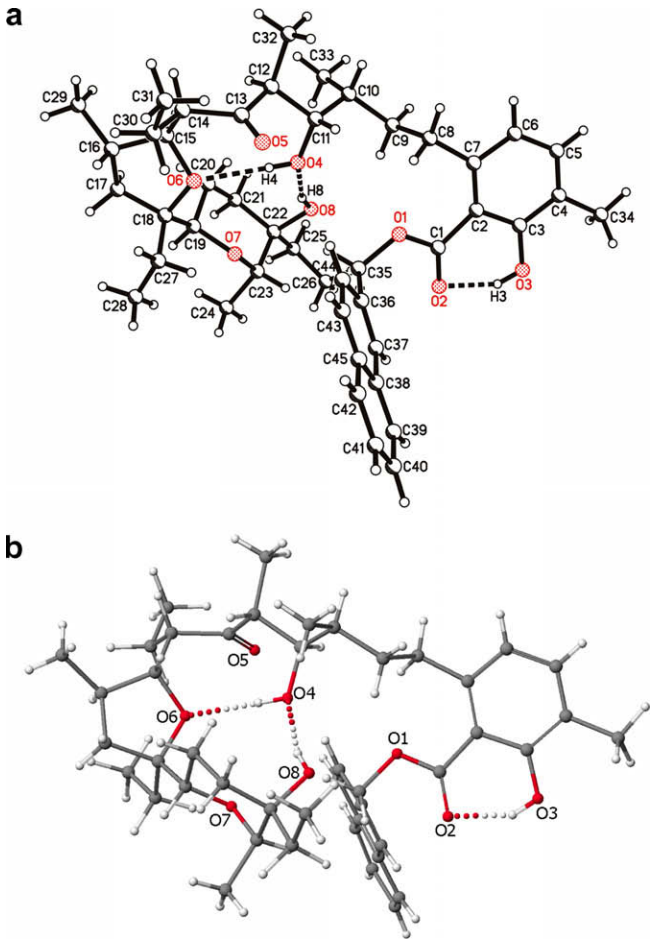

Fig. 1. (a) A perspective view of NAFB in the crystal structure. Hydrogen bonds have been indicated by dashed lines; (b) The structures of NAFB without the engagement of the C=O carbonyl group in hydrogen bond (type A), calculated by semiempirical PM5 method (WinMopac 2003).

the emission spectra, *n* is the refractive index of solution, the index (S) means sample and (R) means reference. The standard fluorophore for the quantum yield measurements was Quinine sulphate in 0.2 mol dm^{-3} H_2SO_4 ($\Phi^R = 0.51$) [27].

2.6. Semiempirical calculations

PM5 semiempirical calculations were performed using the WinMopac 2003 program. In all cases full geometry optimisation of NAFB was carried out without any symmetry constraints [28–32].

2.7. Elemental analysis

The elemental analysis of NAFB was carried out on Vario ELIII (Elementar, Germany).

2.8. Melting point

Corrected melting point was determined on a Mettler FP900.

3. Results and discussion

The structures and the numbering of the atoms of NAFB are shown in Scheme 1.

3.1. X-Ray structure analysis

NAFB crystallizes as a non-solvate in acetonitrile solution. The molecular dimensions (Table 3) fully confirm the chemical formula of the substance. Three intramolecular hydrogen bonds are characteristic of all the NAFB structures (Table 5). The very short O(3)···O(2) bond (Table 4) is likely to stabilize the nearly coplanar conformation of the C(1)O(1)O(2) group and phenyl ring C(2–7). This hydrogen bond is resonance assisted in the system of conjugated π-electron bonds. A considerable distortion of planarity – the torsion angle O(2)C(1)C(2)C(3) is 12.5(8)° (Table 4) – is due to the overcrowding effect, as also testified by the strongly bent OH···O angle. The other hydrogen bonds, between O(8)H···O(4)H and O(4)HO(6) groups are considerably longer. The intramolecular hydrogen bonds, O(3)H···O(2), O(4)H···O(6) and O(8)H···O(4), are strong stabilizing effects of the molecular conformation in the crystal. In this conformation the carbonyl group C=O(5) is not involved in any hydrogen bonds, which is consistent with the balance of H-donors and H-acceptors in this structure, and with the close location of O(5) to the potential donor hydroxyl group – O(4)H. Due to their close location the potential O(4)H···O(5) bond would be strongly strained. However the formation of the O(4)H···O(5) bond is possible and would considerably change the molecular conformation as has been shown by the semiempirical calculations presented below (Section 3.5). There are no strong intermolecular hydrogen bonds in this crystal structure (Fig. 3 and Table 5).

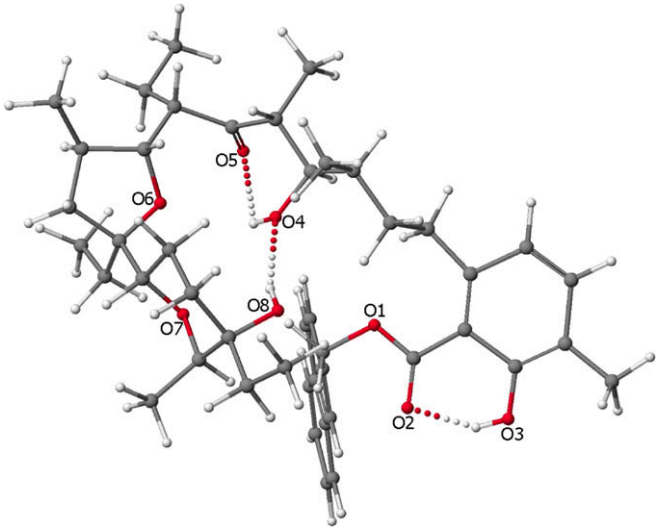

Fig. 2. The structures of NAFB with the engagement of the C=O carbonyl group in hydrogen bond (type B) calculated by the semiempirical PM5 method (WinMopac 2003).

3.2. NMR measurements

The ^1H and ^{13}C NMR data of NAFB are collected in Table 6. In the ^1H NMR spectrum of NAFB in $CDCl_3$ solution the most significantly shifted signal at 11.47 ppm is assigned to the donor proton of the O(3)H group at the salicylic ring involved in the intramolecular O(3)H···O(2)=C hydrogen bond. The signal of the O(4)H and

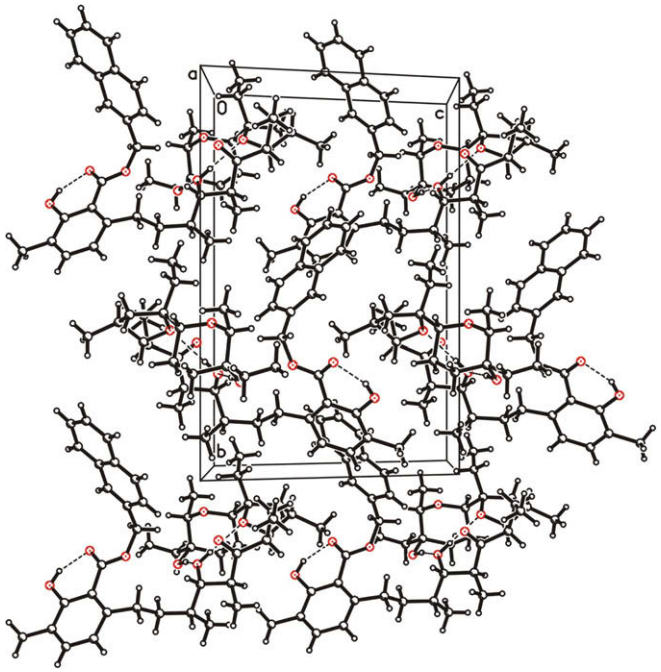

Fig. 3. Arrangement of complex NAFB in the crystal lattice, projected along the [1 0 0] crystal direction.

Table 5
The parameters (length and angle) of intramolecular hydrogen bonds of NAFB determined from X-ray studies and calculated by PM5 semiempirical method

Used method	Compound	Atoms engaged in hydrogen bonds	Length (Å)	Angle (°)
X-ray	$NAFB_{(type\ A\ -\ crystal)}$	O(3)–H···O(2)	2.509(6)	149
		O(8)–H···O(4)	2.874(4)	165
		O(4)–H···O(6)	2.912(4)	179
PM5	$NAFB_{(type\ A)}$	O(3)–H···O(2)	2.60	145
		O(8)–H···O(4)	2.85	160
		O(4)–H···O(6)	2.95	171
	$NAFB_{(type\ B)}$	O(3)–H···O(2)	2.60	145
		O(8)–H···O(4)	2.84	127
		O(4)–H···O(5)	2.90	149

(type A), structure of NAFB in which the C(13)=O group is not engaged in hydrogen bond.
(type B), structure of NAFB in which the C(13)=O group is engaged in hydrogen bond.

Table 6
^{1}H NMR and ^{13}C NMR chemical shifts (ppm) of NAFB in $CDCl_3$

No. atom	^{1}H NMR	^{13}C NMR
1	–	171.80
2	–	111.06
3	–	160.86
4	–	124.04
5	7.16	135.16
6	6.65	121.76
7	–	143.63
8	2.81	34.04
9	1.44–1.68	36.37
10	1.18	33.71
11	3.43	71.46
12	2.72	49.26
13	–	215.05
14	2.70	54.70
15	3.77	85.01
16	2.20	35.04
17	1.51–1.81	39.22
18	–	85.81
19	3.78	73.33
20	1.42–1.64	20.94
21	1.36–1.42	29.98
22	–	70.50
23	3.76	76.57
24	1.16	14.05
25	1.58	29.34
26	0.88	6.41
27	1.29	30.61
28	0.80	8.45
29	1.00	15.97
30	1.34–1.81	18.21
31	0.66	12.23
32	0.55	12.94
33	0.84	12.68
34	2.21	15.86
35	5.56	67.61
36	–	133.22
37	7.91	133.14
38	–	133.14
39	~7.85	128.28
40	7.49	127.67
41	7.55	126.30
42	~7.85	127.67
43	~7.85	128.54
44	7.47	127.47
45	–	132.52
O(3)H	11.47	–
O(4)H	3.28	–
O(8)H	3.28	–

O(8)H protons arises as one broadened signal at 3.28 ppm indicating that both protons are involved in relatively weak hydrogen bonds.

The signals of the naphthalene ring protons are found in the range between 7.47–7.91 ppm, whereas the C(5)H and C(6)H proton signals of the salicylic moiety arise as two doublets at 7.16 and 6.65 ppm, respectively (Fig. 4). The signal of the methylene group protons is observed at 5.56 ppm as a doublet of doublets due to the geminal (^{2}J) spin–spin coupling (Fig. 4). This kind of coupling indicates that both protons are located in different electronic environments and a typical AB spin–spin coupling structure is observed.

The most interesting signals in the ^{13}C NMR spectrum of NAFB are those of C(1) and C(3) carbon atoms, which suggest the existence of enol and/or ketol tautomeric forms of the lasalocid esters. These signals arise at 171.80 ppm and 160.86 ppm, respectively, indicating that NAFB exists in solution predominantly in the enol form as shown in Scheme 1.

3.3. FT-IR measurements

In Fig. 5a and b, the spectra of NAFB in chloroform (dashed line) and in KBr (solid line) are compared. In the spectrum of NAFB in KBr only one band assigned to the ν(OH) vibrations of O(4)H and O(8)H groups is observed at 3448 cm^{-1} indicating that these OH groups form relatively weak hydrogen bonds of comparable strength. This observation is in good agreement with the X-ray structure of NAFB. The vibration of the proton in the intramolecular O–H···O=C hydrogen bond, which is the strongest of all hydrogen bonds should be observed in the FT-IR spectrum in the region below 3000 cm^{-1}. However, this absorption does appear very clearly neither in the NAFB solid state spectrum nor in the spectrum of chloroform solution. The reason for the low intensity of this absorption is probably a strong coupling of the proton motion in the intramolecular hydrogen bond with the π-electrons within the pseudo-aromatic structure which results in a loss of proton polarizability [33].

In the spectrum of NAFB in chloroform solution a broad band with a maximum at about 3443 cm^{-1} and a new weak one at about 3580 cm^{-1} are observed (Fig. 5a, dashed line). The latter band indicates that in chloroform solution one of the weak hydrogen bonds is partially broken. This indicates that the structure of NAFB undergoes slight changes in solution as compared to the solid state. A similar conclusion can be drawn from the spectra in the region of the ν(C=O) vibrations (Fig. 5b). It is obvious, that the NAFB spectrum of the solid state (solid line) exhibits only one band at 1715 cm^{-1} assigned to the ν(C=O) vibrations of C(13)=O group. However, in chloroform solution the intensity of this band decreases and an additional shoulder at 1702 cm^{-1} arises. The existence of the shoulder at 1702 cm^{-1} indicates that in chloroform solution the keto C(13)=O group becomes partially hydrogen-bonded. This supports the statement that the solution structure of NAFB is slightly different compared to the solid state structure.

Furthermore, the band characteristic of the ester group at about 1650 cm^{-1} seems to be unchanged in both states.

3.4. UV–vis and fluorescence studies

The absorption and emission spectra of NAFB are shown in Fig. 6 and the spectral characteristics are given in Table 7. In the

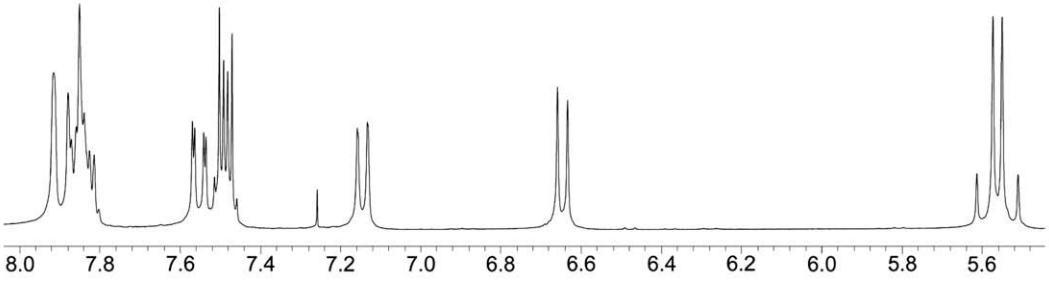

Fig. 4. ^{1}H NMR spectrum of NAFB in region of aromatic proton signals.

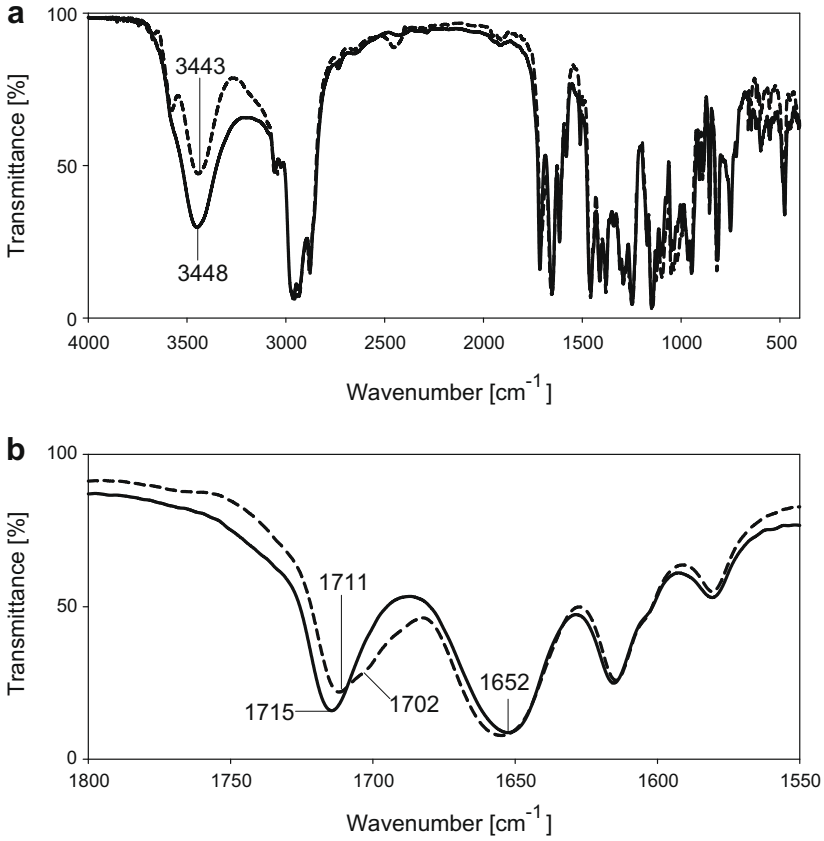

Fig. 5. FT-IR spectra of NAFB: (—) in KBr pallet, (- - -) in chloroform: (a) 4000–400 cm^{-1}; (b) 1800–1550 cm^{-1}.

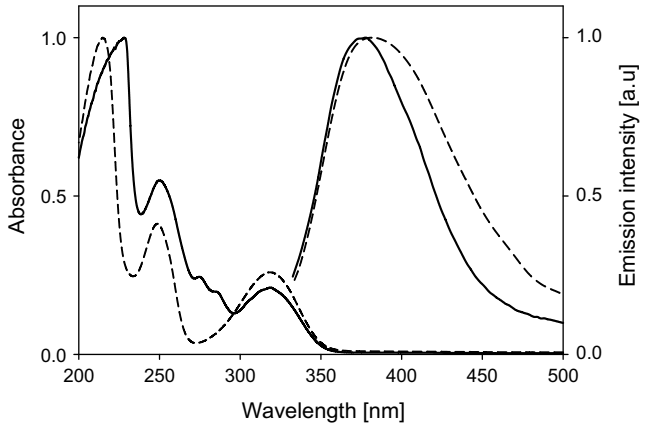

Fig. 6. Absorption (left) and emission corrected spectra (right) of: NAFB (—) and LAS (- - -).

Table 7
UV–vis and fluorescence spectral characteristics of NAFB

UV–vis		Fluorescence		
λ_{max} (nm)	Log ε	λ_{exc} (nm)	λ_{em} (nm)	Φ
228.0	4.41	260	378	3.7×10^{-2}
250.0	4.15			
274.5	3.80			
286.0	3.70			
318.5	3.73			

λ_{max}, maximum of the absorption band; ε, molar extinction coefficient (dm^{-3} mol^{-1} cm^{-1}); λ_{exc}, excitation wavelength; λ_{em}, maximum of the fluorescence band; Φ, quantum yield of fluorescence relative to Quinine sulphate in 0.1 N H_2SO_4 [27].

absorption spectrum of NAFB an intense band at 226 nm together with less intense satellite bands in the region 260–350 nm are observed (Fig. 6 left, solid line). The absorption maxima at 274 and 286 nm in the UV–vis spectrum of NAFB is caused by π–π^* transitions in the naphthalene ring. The respective spectrum of lasalocid acid is less structured. Only three bands with maxima at 215 nm, 248 nm and 318 nm (Fig. 6, dashed line) are observed. The fluorescence spectrum of NAFB shows a band with a maximum at ca. 378 nm (λ_{exc} = 260 nm) (Fig 6 right, solid line). In the fluorescence emission spectrum of lasalocid acid this band is shifted to 381 nm (λ_{exc} = 260 nm) (Fig 6 right, dashed line). The quantum yield of the fluorescence emission of lasalocid acid was calculated to be Φ = 0.15, which is quite high. Note that the salicylic acid moiety of the lasalocid molecule actively contributes to the emission [34]. In contrast, the new 2-naphthylmethyl ester of lasalocid acid shows a two orders of magnitude lower quantum yield of fluorescence (Table 7), which indicates an influence of the carboxylic group on this process.

3.5. PM5 calculations

On the basis of the spectroscopic as well as X-ray results, the structure of NAFB (type A) was calculated by the PM5 semiempirical method and compared to the crystal structure (Fig. 1). The hydrogen bond parameters of NAFB are collected in Table 5 together with the respective X-ray data. On the basis of the spectroscopic observations the respective structure of NAFB was calculated (type B structure, Fig. 2). In this structure the C(13)═O is involved in the formation of an intramolecular hydrogen bond.

The calculated hydrogen bond parameters for the type A structure are comparable with those determined by the X-ray method, although these two methods describe two different states, i.e. the

gas and the solid state, which indicates that the PM5 semiempirical method is a reliable tool for visualization of structures also in the solid state.

The structure of NAFB (B type) is stabilized by the formation of three intramolecular hydrogen bonds that cause the formation of two different parts of the ester molecule (Table 5). One part includes the salicylic group and is stabilized by the O(3)···O(2) intramolecular hydrogen bond. The rest of the molecule is stabilized by two O(8)–H···O(4) and O(4)–H···O(5)═C(13) intramolecular hydrogen bonds.

Acknowledgement

Dr. Adam Huczyński wishes to thank the Foundation for Polish Science for a fellowship.

References

[1] J.W. Westley, J. Antibiot. 29 (1974) 584.
[2] S. Lindenbaum, L. Sternson, S. Rippel, J. Chem. Soc., Chem. Commun. (1977) 268.
[3] M. Schadt, G. Haeusler, J. Membr. Biol. 18 (1974) 277.
[4] J. Bolte, C. Demuynck, G. Jeminet, J. Juilard, C. Tissier, Can. J. Chem. 60 (1982) 9821.
[5] L. Blau, R.B. Stern, R. Bittman, Biochim. Biophys. Acta 778 (1984) 219.
[6] Y.N. Antonenko, L.S. Yaguzhinski, FEBS Lett. 163 (1983) 42.
[7] J.G.D. Phillies, H.E. Stanley, J. Am. Chem. Soc. 98 (1976) 3892.
[8] D.J. Patel, C. Shen, Proc. Natl. Acad. Sci. USA 73 (1976) 4277.
[9] C.C. Chiang, I.C. Paul, Science 196 (1977) 1441.
[10] E.C. Bissell, I.C. Paul, J. Chem. Soc., Chem. Commun. (1972) 967.
[11] J. Berger, A.I. Rachlin, W.E. Scott, L.H. Sternbach, M.W. Goldberg, J. Am. Chem. Soc. 73 (1951) 5295.
[12] V.C. Langston, F. Galey, R. Lovell, W.B. Buck, Vet. Med. 80 (1985) 75–84.
[13] Y. Miyazaki, M. Shibuya, M. Sugasawa, O. Kawaguchi, C. Hirose, J. Nagatsu, S. Esumi, J. Antibiot. 27 (1974) 814.
[14] B.C. Granzim, G.McL. Dryden, Anim. Feed Sci. Technol. 120 (2005) 116.
[15] V. Rada, M. Marounek, Ann. Zeotechnol. 45 (1996) 283.
[16] B. Kohler, H. Karch, H. Schmidt, Microbiology 146 (2000) 1085.
[17] H. Tsukube, Cation-binding by Macrocycles, Marcel-Dekker, New York, 1990.
[18] R. Pankiewicz, G. Schroeder, B. Brzezinski, F. Bartl, J. Mol. Struct. 699 (2004) 53.
[19] R. Pankiewicz, G. Schroeder, B. Brzezinski, F. Bartl, J. Mol. Struct. 749 (2005) 128.
[20] R. Pankiewicz, G. Schroeder, B. Brzezinski, J. Mol. Struct. 733 (2005) 217.
[21] R. Pankiewicz, G. Schroeder, B. Brzezinski, J. Mol. Struct. 733 (2005) 155.
[22] A. Huczyński, R. Wawrzyn, B. Brzezinski, F. Bartl, J. Mol. Struct. 889 (2008) 72.
[23] A. Huczyński, T. Pospieszny, R. Wawrzyn, M. Ratajczak-Sitarz, A. Katrusiak, B. Brzezinski, F. Bartl, J. Mol. Struct. 877 (2008) 105.
[24] A. Huczyński, I. Paluch, M. Ratajczak-Sitarz, A. Katrusiak, J. Stefańska, B. Brzezinski, F. Bartl, J. Mol. Struct. 891 (2008) 481.
[25] G. Sheldrick, SHELXS-97. Program for Crystal Structure Solution, University of Göttingen, 1997.
[26] G. Sheldrick, SHELXL-97. Program for Crystal Structure Refinement, University of Göttingen, 1997.
[27] S.R. Meech, D. Phillips, J. Photochem. 23 (1983) 193.
[28] J.J.P. Stewart, Methods J. Comp. Chem. 10 (1989) 209.
[29] J.J.P. Stewart, J. Comp. Chem. 12 (1991) 320.
[30] A. Huczyński, M. Ratajczak-Sitarz, A. Katrusiak, B. Brzezinski, J. Mol. Struct. 832 (2007) 84.
[31] CAChe 5.04 UserGuide, Fujitsu, 2003.
[32] P. Przybylski, A. Huczyński, B. Brzezinski, J. Mol. Struct. 826 (2007) 156.
[33] L. Sobczyk, S.J. Grabowski, T.M. Krygowski, Chem. Rev. 105 (2005) 3513.
[34] F.S. Richardson, A.D. Gupta, J. Am. Chem. Soc. 103 (1981) 5716.